NASA Technical Memorandum 4753

Multilayer Analyses of an Iron Radiation Beam Experiment

J. L. Shinn and J. W. Wilson
Langley Research Center • Hampton, Virginia

E. V. Benton
University of San Francisco • San Francisco, California

F. F. Badavi
Christopher Newport University • Newport News, Virginia

National Aeronautics and Space Administration
Langley Research Center • Hampton, Virginia 23681-0001

April 1997

Acknowledgments

E. V. Benton would like to thank Walter Schimmerling of NASA Headquarters for suggesting our involvement in the fragmentation work and Jack Miller of UC-LBL and his group for sharing their Bevalac beam time and for their help during the irradiations. The portion of the work performed at the University of San Francisco was supported partially by NASA grants NAG9-235 and NAGW-4154.

Available electronically at the following URL address: http://techreports.larc.nasa.gov/ltrs/ltrs.html

Printed copies available from the following:

NASA Center for AeroSpace Information
800 Elkridge Landing Road
Linthicum Heights, MD 21090-2934
(301) 621-0390

National Technical Information Service (NTIS)
5285 Port Royal Road
Springfield, VA 22161-2171
(703) 487-4650

Abstract

A nonperturbative analytic solution of Green's function for heavy ion transport in a single medium is extended to multilayer transport media. This extension is implemented in the Green's function code (GRNTRN), which is being validated with laboratory experiments. Good agreement is achieved between an iron radiation beam experiment and GRNTRN only when the interactions of the iron radiation beam with several important layers of material located upstream of the target within the beamline are considered.

Introduction

Astronauts and occupants of high-altitude aircraft are exposed to heavy-ion cosmic radiation that originates from the Sun and galactic sources. The shielding and exposure of these individuals are controlled by the transport properties of the radiation through the specific materials. Efficient space-radiation-transport computer codes (refs. 1, 2, and 3) have been developed and applied to a wide range of missions, but the results of these codes could not be validated accurately in laboratory experiments (ref. 4). Recently, the use of a nonperturbative approach to Green's function solutions has led to an efficient laboratory code, namely, Green's function transport (GRNTRN) code (ref. 5), which will be further developed for space-radiation-transport calculations and validated with laboratory experiments.

Preliminary validation of the laboratory Green's function code (GRNTRN) has been made by comparing the theoretical results with recent iron radiation beam measurements made at Lawrence Berkeley Laboratory Bevalac accelerator by Shinn et al. (ref. 6). The iron beam had been accelerated to 600 MeV/amu and passed through a series of beam-transport elements, triggering devices, and a lead-foil beam spreader prior to emerging from the beam tube and striking a layer of aluminum or polyethylene targets. Overall, fairly good agreement between measurements and predictions from GRNTRN was reached when the nuclear database used in GRNTRN was improved in the physical formulation and corrected for mass and charge conservation (refs. 7 and 8). Furthermore, as the code was modified to include the interactions of beam and lead foil, better agreement was reached except that the predicted fragmentation was still low by 30 percent for the aluminum target. The code modification was made to extend the nonperturbative solutions for a single medium to inhomogeneous, two-layer transport media (for lead foil and target material). In this paper, we present further improvement to our analytical results by modifying GRNTRN to include interactions from other significant layers of material from the beam tube. The development of the nonperturbative method to inhomogeneous, multilayer (three or more layers) transport media will be given with a brief review of the analytic properties of the perturbative solution of the heavy-ion-propagation problem and a nonperturbative approximation to the full perturbation series.

Transport Equation

We restrict our attention to the multiple charged ions for which the Boltzmann equation may be reduced (ref. 9) to

$$\left[\frac{\partial}{\partial x} - \frac{\partial}{\partial E}\tilde{S}_j(E) + \sigma_j\right]\phi_j(x, E) = \sum_k \sigma_{jk}\phi_k(x, E) \tag{1}$$

where $\phi_j(x,E)$ is the flux of ion type j at x with energy E (in MeV/amu), $\tilde{S}_j(E)$ is the change in E per unit distance, σ_j is the total macroscopic reaction cross section, and σ_{jk} is the macroscopic cross section for

collision of ion type k to produce an ion of type j. The solution to equation (1) is to be found subject to the boundary condition

$$\phi_j(0,E) = f_j(E) \tag{2}$$

The corresponding Green's function is introduced as a solution of

$$\left[\frac{\partial}{\partial x} - \frac{\partial}{\partial E}\tilde{S}_j(E) + \sigma_j\right] G_{jm}(x, E, E') = \sum_k \sigma_{jk} G_{km}(x, E, E') \tag{3}$$

subject to the boundary condition that $G_{jm}(0, E, E') = \delta_{jm}\delta(E - E')$.

The preceding equations can be simplified by transforming the energy into the residual range as

$$r_j = \int_0^E \frac{dE'}{\tilde{S}_j(E')} \tag{4}$$

and defining new field functions as

$$\psi_j(x, r_j) = \tilde{S}_j(E)\phi_j(x, E) \tag{5}$$

$$G_{jm}(x, r_j, r'_m) = \tilde{S}_j(E) G_{jm}(x, E, E') \tag{6}$$

$$\hat{f}_j(r_j) = \tilde{S}_j(E)\phi_j(0, E) \tag{7}$$

Equation (3) becomes

$$\left(\frac{\partial}{\partial x} - \frac{\partial}{\partial r_j} + \sigma_j\right) G_{jm}(x, r_j, r'_m) = \sum_k \frac{\nu_j}{\nu_k} \sigma_{jk} G_{km}(x, r_k, r'_m) \tag{8}$$

with the boundary condition

$$G_{jm}(0, r_j, r'_m) = \delta_{jm}\delta(r_j - r'_m) \tag{9}$$

and with the solution to the ion fields given by

$$\psi_j(x, r_j) = \sum_m \int_0^\infty G_{jm}(x, r_j, r'_m)\hat{f}_m(r'_m)\, dr'_m \tag{10}$$

Note that ν_j is the range scale factor such that $\nu_j r_j = \nu_m r_m$ and can be taken as $\nu_j = Z_j^2/A_j$.

Perturbative Green's Function

The solution to equation (8) is written as a perturbation series:

$$G_{jm}(x, r_j, r'_m) = \sum_i G_{jm}^{(i)}(x, r_j, r'_m) \tag{11}$$

where

$$G_{jm}^{(0)}(x, r_j, r'_m) = \exp(-\sigma_j x)\delta_{jm}\delta(x + r_j - r'_m) \tag{12}$$

and the first collision term is

$$G_{jm}^{(1)}(x, r_j, r'_m) = \frac{\nu_j \sigma_{jm}}{|\nu_m - \nu_j|} \exp(-\sigma_j x_j - \sigma_m x_m) \tag{13}$$

where $G_{jm}^{(1)}(x, r_j, r'_m)$ takes on nonzero values for

$$\frac{\nu_j}{\nu_m}(r_j + x) \le r'_m \le \frac{\nu_j}{\nu_m} r_j + x \tag{14}$$

and

$$x_j = (\nu_m x + \nu_j r_j - \nu_m r'_m)/(\nu_m - \nu_j) \tag{15}$$

$$x_m = (\nu_m r'_m - \nu_j x - \nu_j r_j)/(\nu_m - \nu_j) \tag{16}$$

Note that in equations (13)–(16), $x_j + x_m = x$ for all r_j and r'. The significance of x_m is that it is the distance ion m traveled from the boundary to the collision site at which the ion j was produced and must now travel distance x_j before reaching x. Similar results hold for higher order terms (refs. 10 and 11).

Whenever $r_j, r'_m < x$, it is relatively easy to show that

$$\int_{r_{jl}}^{r_{ju}} G_{jm}^{(1)}(x, r_j, r'_m) dr_j = \sigma_{jm} g(j, m) \tag{17}$$

where the integral limits are the interval limits in equation (14) and $g(j, m)$ is the g-function of two arguments defined by the following relations:

$$g(j) = \exp(-\sigma_j x) \tag{18}$$

and

$$g(j_1, j_2, \ldots, j_n, j_{n+1}) = \frac{g(j_1, j_2, \ldots, j_{n-1}, j_n) - g(j_1, j_2, \ldots, j_{n-1}, j_{n+1})}{\sigma_{jn+1} - \sigma_{jn}} \tag{19}$$

The first collision Green's function term may be approximated by the spectral averaged value as

$$\begin{aligned} G_{jm}^{(1)}(x, r_j, r'_m) &\approx \frac{1}{r_{ju} - r_{jl}} \int_{r_{jl}}^{r_{ju}} G_{jm}^{(1)}(x, r_j, r_m)\, dr_j \\ &= \frac{\nu_j \sigma_{jm} g(j, m)}{x|\nu_m - \nu_j|} \end{aligned} \tag{20}$$

and is functionally dependent only on depth of penetration x. Its contribution applies only over the energy range of equation (14) and is null outside. The higher order terms are approximated by their spectral averages as

$$G_{jm}^{(i)}(x, r_j, r'_m) \approx \sum_{k_1, k_2, \ldots, k_{i-1}} \frac{\nu_j \sigma_{jk_1} \sigma_{k_1 k_2} \cdots \sigma_{k_{i-1} m} g(j, k_1, k_2, \ldots, k_{i-1}, m)}{x|\nu_m - \nu_j|} \tag{21}$$

Note that $G_{jm}^{(i)}(x, r_j, r'_m)$ is purely dependent on x for $i > 0$, and we represent the expression as $G_{jm}^{(i)}(x)$ (ref. 4). In terms of equations (11)–(21), the solution to equation (1) becomes (ref. 4)

$$\psi_j(x, r_j) = \exp(-\sigma_j x)\hat{f}_j(r_j + x) + \sum_{m,i} G_{jm}^{(i)}(x)\left[\hat{F}'_m(r'_{ml}) - \hat{F}_m(r'_{mu})\right] \tag{22}$$

In equation (22), $r'_{m,u}$ and $r'_{m,l}$ are given by the upper and lower limits of the r'_m, satisfying equation (14). The symbol $\hat{F}_m(r'_m)$ refers to the integral spectrum

$$\hat{F}_m(r'_m) = \int_{r'_m}^{\infty} \hat{f}m(r)\, dr \tag{23}$$

Nonperturbative Green's Function

We now introduce nonperturbation terms for the summation in equation (22). First, we note that

$$g_{jm}(x) = \delta_{jm}g(m) + \sigma_{jm}g(j, m) + \sum_k \sigma_{jk}\sigma_{km}g(j, k, m) + \ldots \tag{24}$$

A term-by-term comparison of the series (22) with the series (9) shows that, in the spectral average approximation, we may write the approximate solution as

$$\psi_j(x, r_j) = \exp(-\sigma_j x)\hat{f}(r_j + x) + \sum_m \frac{\nu_j[g_{jm}(x) - \exp(-\sigma_j x)\delta_{jm}]}{x|\nu_m - \nu_j|}\left[\hat{F}_m(r'_{mu}) - \hat{F}_m(r'_{ml})\right] \tag{25}$$

which is a relatively simple quantity once $g_{jm}(x)$ is evaluated (ref. 4). The advantage of equation (23) is that $g_{jm}(x)$ satisfies the convolution product relation (ref. 12) as

$$g_{jm}(x) = \sum_k g_{jk}(x - y)g_{km}(y) \tag{26}$$

for any positive values of x and y. A solution for small x is easily obtained from the first few terms of equation (24). Equation (26) may then be used to propagate the function $g_{jm}(x)$ over the entire solution space, taking arbitrarily large steps.

Nonperturbative Method for a Shielded Medium

The major simplification in the Green's function method results from the fact that the scaled spectral distribution of secondary ions to a first approximation depends only on the depth of penetration, as seen in equations (20), (21), and (22). Our first approach to a multilayered Green's function will rely on this observation and assume its validity for multilayered shields.

Consider a domain labeled as 1 that is shielded by a second domain labeled as 2; the number of type j ions at depth x in 1 due to type m ions incident on domain 2 of thickness y is

$$g_{12jm}(x, y) = \sum_k g_{1jk}(x)g_{2km}(y) \tag{27}$$

The leading term in equation (24) is the penetrating primaries as

$$g_{12jm}(x, y) = \exp(-\sigma_{1j}x - \sigma_{2j}y)\delta_{jm} + [g_{12jm}(x, y) - \exp(-\sigma_{1j}x - \sigma_{2j}y)\delta_{jm}] \tag{28}$$

where all higher order terms are in the bracket of equation (28). The first term of the scaled Green's function is then

$$G^{(0)}_{12jm}(x, y, r_j, r'_m) = \exp(-\sigma_{1j}x - \sigma_{2j}y)\delta_{jm}\delta[x + r_j - (r'_m - \rho y)] \tag{29}$$

where ρ is the range scale factor for the two media

$$\rho = R_{1j}(E)/R_{2j}(E) \tag{30}$$

which is fairly constant above 10 MeV/amu or so. We take a single value for ρ that corresponds to 600 MeV/amu. The secondary contribution is similarly found from equation (14) as

$$\frac{\nu_j}{\nu_m}(r_j + x + \rho y) \le r'_m \le \frac{\nu_j}{\nu_m} r_j + x + \rho y \tag{31}$$

from which the average spectrum is evaluated. The full approximate Green's function is then

$$\begin{aligned} G_{12jm}(x, y, r_j, r'_m) \approx{}& \exp(-\sigma_{1j}x - \sigma_{2j}y)\delta_{jm}\delta(x + \rho y + r_j - r'_m) \\ &+ \frac{\nu_j[g_{12jm}(x, y) - \exp(-\sigma_{1j}x - \sigma_{2j}y)\delta_{jm}]}{(x + \rho y)|\nu_m - \nu_j|} \end{aligned} \tag{32}$$

Equation (32) is our first approximation of Green's function in a shielded medium of two layers, and is easily modified to multiple layers. (See appendix.)

For the first spectral modification, the first collision term has the properties

$$G^{(1)}_{12jm}(x, y, r_j, r'_m) = \left\{ \begin{array}{ll} \dfrac{\nu_j \sigma_{1jm} \exp(-\sigma_{1m}x - \sigma_{2m}y)}{|\nu_m - \nu_j|} & r'_m = r'_{mu} \\ \dfrac{\nu_j \sigma_{2jm} \exp(-\sigma_{1j}x - \sigma_{2j}y)}{|\nu_m - \nu_j|} & r'_m = r'_{ml} \end{array} \right\} \tag{33}$$

These properties are used to correct the average spectrum to

$$G^{(1)}_{12jm}(x, y, r_j, r'_m) = \frac{\nu_j g^{(1)}_{12jm}(x, y)}{(x + \rho y)|\nu_m - \nu_j|} + b_{jm}(x, y)(r'_m - \bar{r}_m) \tag{34}$$

where $g^{(1)}_{12jm}(x, y)$ is the first collision term of equation (32) and

$$\bar{r}'_m = \frac{r'_{mu} + r'_{ml}}{2} \tag{35}$$

is the midpoint of $\bar{r}'_m$ between its limits given by equation (31). The b_{jm} term of equation (34) has the property that

$$\int_{r'_{ml}}^{r'_{mu}} b_{jm}(x, y)(r' - \bar{r}'_m)\, dr' = 0 \tag{36}$$

which ensures that the first term of equation (34) is indeed the average spectrum as required. The spectral slope parameter is

$$b_{jm}(x, y) = \frac{\nu_j \nu_m [\sigma_{1jm} \exp(-\sigma_{1m} x - \sigma_{2m} y) - \sigma_{2jm} \exp(-\sigma_{1j} x - \sigma_{2j} y)]}{(x + \rho y)(\nu_m - \nu_j)|\nu_m - \nu_j|} \tag{37}$$

A similarly simple spectral correction could be made to the higher order terms. The spectral correction given in equation (37) is included in the present Green's function code.

Spectra for Laboratory Beams

The boundary condition appropriate for laboratory beams is given by

$$f_j(E) = \frac{1}{\sqrt{2\pi}\sigma} \exp\left[\frac{-(E - E_0)^2}{2\sigma^2}\right] \tag{38}$$

where E_0 is the mean energy of beam with an energy spread σ. The cumulative spectrum is given by

$$F_j(E) = \frac{1}{2}\left[1 - erf\left(\frac{E - E_0}{\sqrt{2}\sigma}\right)\right] \tag{39}$$

The cumulative energy moment needed to evaluate the spectral correction is

$$\bar{E}_j(E) = \frac{1}{2}E_0\left[1 - erf\left(\frac{E - E_0}{\sqrt{2}\sigma}\right)\right] + \frac{\sigma}{\sqrt{2\pi}} \exp\left[-\frac{(E - E_0)^2}{2\sigma^2}\right] \tag{40}$$

The average energy on any subinterval (E_1, E_2) is then

$$\bar{E} = \frac{\bar{E}_j(E_1) - \bar{E}_j(E_2)}{F_j(E_1) - F_j(E_2)} \tag{41}$$

The beam generated flux is

$$\begin{aligned} \psi_j(x, y, r_j) = {} & \exp(-\sigma_{1j} x - \sigma_{2j} y) \hat{f}_j(r_j + x + \rho y) \\ & + \sum_{m, i} G^{(i)}_{jm}(x, y)[\hat{F}_m(r'_{mu}) - \hat{F}_m(r'_{ml})] \\ & + \sum_{m} b^{(1)}_{jm}(x, y)[r'_m(\bar{E}) - r'_m][\hat{F}_m(r'_{mu}) - \hat{F}_m(r'_{ml})] \end{aligned} \tag{42}$$

where $\bar{E}$ is evaluated with equation (41), with E_1 and E_2 as the lower and upper limits, respectively, associated with r'_{ml} and r'_{mu}.

The linear energy transfer (LET) distributions behind aluminum and polyethylene targets were measured with a stack of four CR-39 plastic nuclear track detectors (PNTD's) placed behind the target (ref. 13). The incident beam intensity was monitored by a thin layer of CR-39 PNTD placed immediately in front of the target. Calibration of these detectors with various ion beams of known LET resulted in a response function that is approximately Gaussian with a LET-dependent width. The detectors and targets were run in good geometry so that acceptance corrections are not required. The detector response function is used to compare the experiment with the calculated LET distributions from GRNTRN, assuming 0.2 percent beam-energy spread in equation (38).

Figures 1(a) and (b) show measured and calculated LET spectra behind 2-g/cm^2 aluminum and 4.6-g/cm^2 polyethylene targets, respectively. The calculations include the interactions between the iron beam and 2.24 g/cm^2 of the "thin" lead-scattering foil placed upstream of the target. The energy of the iron beam prior to its interaction with the two-layer lead-target combination was 557 MeV/amu. The calculated LET spectra for fragments are in good agreement for the polyethylene target experiment (fig. 1(b)), but are 30 percent lower than the measurement for the aluminum target (fig. 1(a)). Note that the spread in each isotope peak results mostly from the detector-response function rather than the beam-energy spread.

Some of the materials used in the beamline, other than lead foil, that could cause significant modifications to the beam prior to its interaction with the target were further identified. In our latest calculation, a 0.16-cm-thick (0.43-g/cm^2) aluminum exit plate and two polystyrene scintillators of 0.16-cm and 0.32-cm thickness (total 0.49 g/cm^2) were included in our transport analyses. Equations (42) and (32) were modified for a four-layer (lead foil, aluminum exit plate, polystyrene, and target) configuration and implemented in GRNTRN. The improved result for the 2-g/cm^2 aluminum target appears in figure 2. For the polyethylene target, the results of a four-layer calculation (not shown) were not appreciably different from those of the two-layer calculation, as was expected. Because the fragmentation for the polyethylene target is far greater than those for the aluminum target, the contributions from the aluminum exit plate and polystyrene are far less significant than those from the lead-foil and polyethylene target. The beam energy for the four-layer shield-target combination was inferred, taking into account the energy loss through these layers, to be 583 MeV/amu. The latter energy value is much closer to the beam energy at extraction (600 MeV/amu), which indicates the four-layer configuration is a good approximation to the exact one.

Concluding Remarks

The iron radiation beam experiment with CR-39 plastic nuclear track detectors (PNTD's) provides a fairly accurate laboratory validation of Green's function transport (GRNTRN) code. Through the multilayer analyses, it is concluded that for thinner targets, the effect of lead-scattering foil, beam-transport elements, and triggering devices in modifying the characteristics of the beam is rather significant. Laboratory validation up to this point provides confidence in the validity of the Green's function method and, in an approximate sense, in the correctness of the nuclear physics theory. Any refinement in the nuclear database used in GRNTRN ultimately will depend on better resolution of each isotope measurement with a state-of-the-art detector system (Zeitlin et al., *Radiat. Meas.*, vol. 23, no. 1, 1994) and more sophisticated analyses, including multilayer configuration.

NASA Langley Research Center
Hampton, VA 23681-0001
December 16, 1996

Appendix

Derivation of Approximate Green's Function for Three-Layer Configuration

The formalism presented in the preceding text is extended to a three-layer configuration as follows. The solution to equation (26) in a three-layered medium is

$$g_{123jm}(x, y, z) = \sum_{kl} g_{1jk}(x) g_{2kl}(y) g_{3lm}(z) \tag{A1}$$

The leading term is the penetrating primaries, and equation (A1) may be written as

$$\begin{aligned} g_{123jm}(x, y, z) = {} & \exp(-\sigma_{1j}x - \sigma_{2j}y - \sigma_{3j}z)\delta_{jm} \\ & + [g_{123jm}(x, y, z) - \exp(\sigma_{1j}x - \sigma_{2j}y - \sigma_{3j}z)\delta_{jm}] \end{aligned} \tag{A2}$$

The scaled Green's function is then

$$\begin{aligned} G_{123jm}(x, y, z, r_j, r'_m) \approx {} & -\exp(-\sigma_{1j}x - \sigma_{2j}y - \sigma_{3j}z)\delta_{jm}\delta(x + \rho_2 y + \rho_3 z + r_j - r'_m) \\ & + \frac{\nu_j[g_{123jm}(x, y, z) - \exp(-\sigma_{1j}x - \sigma_{2j}y - \sigma_{3j}z)\delta_{jm}]}{(x + \rho_2 y + \rho_3 z)(\nu_m - \nu_j)} \end{aligned} \tag{A3}$$

where $\rho_2 = R_{1j}(E)/R_{2j}(E)$ and $\rho_3 = R_{1j}(E)/R_{3j}(E)$. The range condition of equation (17) becomes

$$\frac{\nu_j}{\nu_m}(r_j + x + \rho_2 y + \rho_3 z) \le r'_m \le \frac{\nu_j}{\nu_m} r_j + x + \rho_2 y + \rho_3 z \tag{A4}$$

The spectral corrections are similarly derived.

References

1. Wilson, John W.; Townsend, Lawrence W.; Schimmerling, Walter; Khandelwal, Govind S.; Khan, Ferdous; Nealy, John E.; Cucinotta, Francis A.; Simonsen, Lisa C.; Shinn, Judy L.; and Norbury, John W.: *Transport Methods and Interactions for Space Radiations*. NASA RP-1257, 1991.

2. Shinn, Judy L.; and Wilson, John W.: *An Efficient HZETRN (A Galactic Cosmic Ray Transport Code)*. NASA TP-3147, 1992.

3. Wilson, John W.; Chun, Sang Y.; Badavi, Forooz F.; Townsend, Lawrence W.; and Lamkin, Stanley L.: *HZETRN: A Heavy Ion/Nucleon Transport Code for Space Radiations*. NASA TP-3146, 1991.

4. Wilson, J. W.; and Badavi, F. F.: New Directions in Heavy Ion Shielding. *Proceedings of the Topical Meeting on New Horizons on Radiation Protection and Shielding*, American Nuclear Soc., Inc., 1992, pp. 198–202.

5. Wilson, J. W.; Shavers, M. R.; Badavi, F. F.; and Miller, J.: Nonperturbative Methods in HZE Propagation. *Radiat. Res.*, vol. 140, no. 2, 1994, pp. 241–248.

6. Shinn, J. L.; Wilson, J. W.; Badavi, F. F.; Benton, E. V.; Csige, I.; Frank, A. L.; and Benton, E. R.: HZE Beam Transport in Multilayered Materials. *Radiat. Meas.*, vol. 23, no. 1, 1994, pp. 57–64.

7. Shinn, Judy L.; Wilson, John W.; Benton, E. V.; Csige, I.; Frank, A. L.; and Benton, E. R.: *LET Spectra of Fragmented 600 MeV/A Iron Beam on Aluminum and Polyethylene—A Preliminary Analysis*. NASA TP-3436, 1994.

8. Wilson, J. W.; Shinn, J. L.; Townsend, L. W.; and Tripathi, R. K.: NUCFRG2: A Semiempirical Nuclear Fragmentation Model. *Nucl. Instrum. Methods in Phys. Res. B*, vol. 94, 1994, pp. 95–102.

9. Wilson, John W.: *Analysis of the Theory of High-Energy Ion Transport*. NASA TN D-8381, 1977.

10. Wilson, John W.; Townsend, L. W.; Lamkin, S. L.; and Ganapol, B. D.: A Closed-Form Solution to HZE Propagation. *Radiat. Res.*, vol. 122, no. 3, June 1990, pp. 223–228.

11. Wilson, John W.; Townsend, L. W.; Bidasaria, H. B.; Schimmerling, Walter; Wong, Mervyn; and Howard, Jerry: ^{20}Ne Depth-Dose Relations in Water. *Health Phys.*, vol. 46, no. 5, May 1984, pp. 1101–1111.

12. Wilson, John W.; Costen, Robert C.; Shinn, Judy L.; and Badavi, Francis F.: *Green's Function Methods in Heavy Ion Shielding*. NASA TP-3311, 1993.

13. Benton, E. V.; Ogura, K.; Frank, A. L.; Atallah, T.; and Rowe, V.: Response of Different Types of CR-39 to Energetic Ions. *Nucl. Tracks Radiat. Meas.*, vol. 12, 1986, pp. 79–82.

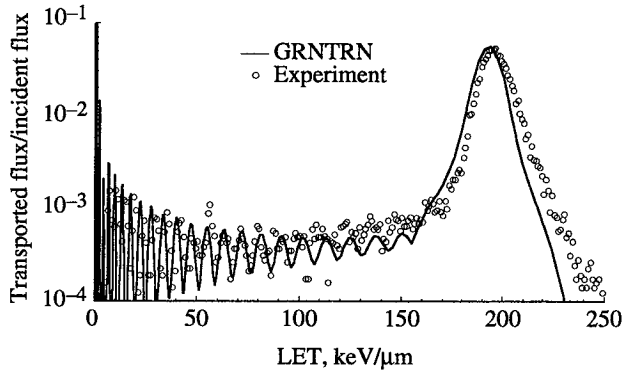

(a) 2.24 g/cm^2 Pb + 2 g/cm^2 Al.

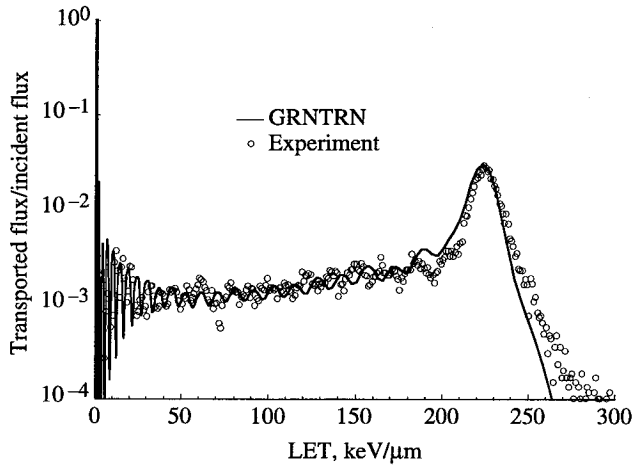

(b) 2.24 g/cm^2 Pb + 4.6 g/cm^2 polyethylene).

Figure 1. Transport measurements and calculations for lead and target (two-layer) combination for 557-MeV/amu iron beam.

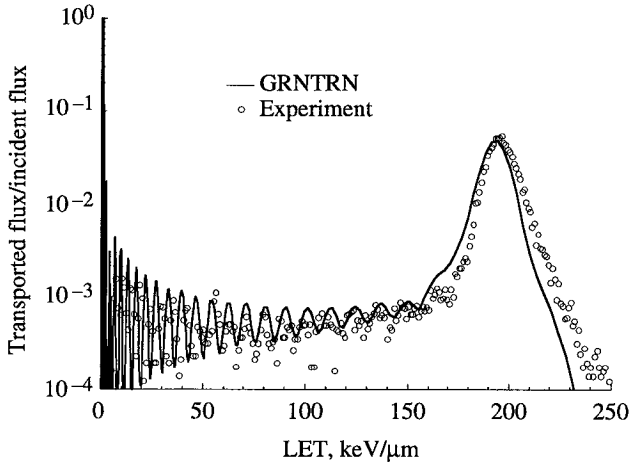

Figure 2. Transport measurements and calculations for four-layer shield and target combination (2.24 g/cm^2 Pb + 0.42 g/cm^2 Al + 0.49 g/cm^2 polystyrene + 2 g/cm^2 Al) for 583-MeV/amu iron beam.

REPORT DOCUMENTATION PAGE

Form Approved
OMB No. 0704-0188

1. AGENCY USE ONLY *(Leave blank)*	2. REPORT DATE	3. REPORT TYPE AND DATES COVERED
	April 1997	Technical Memorandum

4. TITLE AND SUBTITLE
Multilayer Analyses of an Iron Radiation Beam Experiment

5. FUNDING NUMBERS
WU 199-45-16-11

6. AUTHOR(S)
J. L. Shinn, J. W. Wilson, E. V. Benton, and F. F. Badavi

7. PERFORMING ORGANIZATION NAME(S) AND ADDRESS(ES)
NASA Langley Research Center
Hampton, VA 23681-0001

8. PERFORMING ORGANIZATION REPORT NUMBER
L-17586

9. SPONSORING/MONITORING AGENCY NAME(S) AND ADDRESS(ES)
National Aeronautics and Space Administration
Washington, DC 20546-0001

10. SPONSORING/MONITORING AGENCY REPORT NUMBER
NASA TM-4753

11. SUPPLEMENTARY NOTES
Shinn and Wilson: Langley Research Center, Hampton, VA; Benton: University of San Francisco, San Francisco, CA; Badavi: Christopher Newport University, Newport News, VA.

12a. DISTRIBUTION/AVAILABILITY STATEMENT
Unclassified–Unlimited
Subject Category 93
Availability: NASA CASI (301) 621-0390

12b. DISTRIBUTION CODE

13. ABSTRACT *(Maximum 200 words)*
A nonperturbative analytic solution of Green's function for heavy ion transport in a single medium is extended to multilayer transport media. This extension is implemented in the Green's function code (GRNTRN), which is being validated with laboratory experiments. Good agreement is achieved between an iron radiation beam experiment and GRNTRN only when the interactions of the iron radiation beam with several important layers of material located upstream of the target within the beamline are considered.

14. SUBJECT TERMS
Heavy ion transport; Green's function; Etch track detectors

15. NUMBER OF PAGES
11

16. PRICE CODE
A03

17. SECURITY CLASSIFICATION OF REPORT	18. SECURITY CLASSIFICATION OF THIS PAGE	19. SECURITY CLASSIFICATION OF ABSTRACT	20. LIMITATION OF ABSTRACT
Unclassified	Unclassified	Unclassified	